Proceedings of 2004 Korea-Japan Joint Seminar
on Particle Image Velocimetry
POSTECH, Korea, Dec. 9 - 10

# Micro-LIF measurement of microchannel flow

Kyung Chun Kim and Sang Youl Yoon

School of Mechanical Engineering,
Pusan National University,
San30, Jangjeon-dong, Keumjeong-gu, Busan, 609-735, Korea
*kckim@pusan.ac.kr*

***Abstract:*** Measurement of concentration distributions of suspended particles in a micro-channel is out of the most crucial necessities in the area of Lab-on-a-chip to be used for various bio-chemical applications. One most feasible way to measure the concentration field in the micro-channel is using micro-LIF(Laser Induced Fluorescence) method. However, an accurate concentration field at a given cross plane in a micro-channel has not been successfully achieved so far due to various limitations in the light illumination and fluorescence signal detection. The present study demonstrates a novel method to provide an ultra thin laser sheet beam having five(5) microns thickness by use of a micro focus laser line generator. The laser sheet beam illuminates an exact plane of concentration measurement field to increase the signal to noise ratio and considerably reduce the depth uncertainty. Nile Blue A was used as fluorescent dye for the present LIF measurement. The enhancement of the fluorescent intensity signals was performed by a solvent mixture of water (95%) and ethanol (EtOH)/methanol (MeOH) (5%) mixture. To reduce the rms errors resulted from the CCD electronic noise and other sources, an expansion of grid size was attempted from 1×1 to 3×3 or 5×5 pixel data windows and the pertinent signal-to-noise level has been noticeably increased accordingly.

***Keywords:*** Micro-LIF, Micro laser light sheet, fluorescent intensity enhancement, Solvent mixture, Nile Blue A

## 1. Introduction

Advances in micro-technology related to bio-medical and bio-chemical devices are rapidly progressed in these days. Especially, various kinds of micro scale analysis/diagnostic systems called Micro-Total Analysis System (μ-TAS) or Lab-on-a-chip have been successfully developed and appeared in commercial market. Most of the micro-analysis system contains microfluidic devices, which play crucial roles such as transport, accumulation, mixing and reaction of target materials in fluids. Among them, the most important functions are mixing and reaction. So far, numerous micro-mixers and micro-reactors have been designed and applied (Kim et al., (2003), Glasgow and Aubry, (2003), Suzuki and Ho, (2002)). However, an accurate quantitative measurement technique to verify the performance of these devices has not been completely developed yet. Only qualitative approaches using visualization techniques are available. Hence, it seems quite difficult to verify whether the mixer works well, is optimally designed, or efficiently functioning. Consequently, it is necessary to develop quantitative measurement

methods to obtain concentration distributions in fluids inside the microfluidic devices.

Laser Induced Fluorescence (LIF) technique is well established to measure concentration or temperature fields based on the principle that the fluorescence intensity is proportional to the fluorescence dye concentration or that the fluorescence intensity decreases with increasing suspension temperature. Unlike macro systems, however, for micro-system applications it is somewhat cumbersome to get concentration/temperature fields using the LIF technique because of difficulties arising in the laser sheet illumination and low fluorescence signal intensity. For the case of a micro system, the conventional illumination method is the volume illumination flooding a laser beam onto the tiny measurement field. Consequently, most previous attempts have performed using a volume illumination condition. Recently, Shinohara et al. (2003) measured quantitative PH fields in a Y-shape micro-mixer with an assumption that the flow is two-dimensional. Under the volume illumination, contamination of fluorescence intensity from out of focus region can never be completely avoided. Furthermore, most of mixers develop three dimensional flows so that the conventional μ-LIF technique may have inherent limits and excessive measurement errors. In this study, we are trying to apply very thin laser light sheet in lieu of the volume illumination to measure concentration fields quantitatively by using micro-scale Laser Induced Fluorescence (μ-LIF) technique for microfluidic systems.

The low-intensity problem in LIF measurements could be overcome by increasing the detector sensitivity by use of a cooled CCD camera with high dynamic range (12/14/16 bit), but this generally requires substantially higher budget in comparison with the regular CCD Camera. The innovative idea is to intrinsically enhance the fluorescence signal intensity by adding a proper solvent mixture that enhances the photo affinity of the fluorescence dye. Solvent effects on fluorescence phenomena have been well described in many papers of biology and spectroscopy. While, based on the authors literature review, no work has been published in using the solvent effect for microfluidic concentration detection. Grofesik et al. (1995) and Kubinyi et al. (2003) described the fluorescent life times of Nile Blue A and Oxazine 720 dissolved in several pure solvents at different temperatures. Krihak et al. (1997) investigated the absorption and fluorescence wavelength maxima of Nile Blue A and Thionin dissolved in solvents for various polarities and pH values. Ghanadzadeh et al. (2004) reported on the visible absorption spectra of Oxazine dyes (Oxazine 720, Oxazine 750, Nile Blue) in different solvents (dioxine, water, methanol, acetone, 5CB). But solvent effects of fluorophores in solvent mixtures have not been investigated as widely as in pure solvents. Mondal et al. 2003) investigated photophisical characteristics of several fluorophores (Dibucaine, Tetracaine, Procaine) in a solvent mixture of ethanol - water and in reverse micelles.

This study aims to enhance the fluorescence intensity signals by using a mixed solvent or different solvent mixtures for micro-LIF measurements. In addition, a novel illumination method is employed to generate laser sheet with only a few micron thickness. Direct scanning of the ultra thin laser sheet through a transparent micro-channel made by PDMS (Polydimethyl-siloxane) or PMMA (Polymethyl methacrylate) allows the possibility of exact measurement of concentration field inside a micro-channel.

## 2. Fluorescent Intensity Signal Enhancement

### *2.1 Steady-state fluorescence intensity and time-resolved fluorescence intensity*

Fluorescence techniques can be broadly classified into two types of measurements, a steady-state and a time-resolved fluorescence. In the steady-state measurement, a continuous beam of light is used, and the subsequent fluorescence intensity or emission spectrum is measured. The aforementioned LIF measurement is a type of the steady-state fluorescence measurement. The

time-resolved measurement using a pulse of light can be used for measuring the intensity decay such as the fluorescent lifetime. The lifetime and spectrum measurement techniques are reported in numerous papers as useful fluorescent information. It is important to understand a simple relationship between the steady-state intensity and the time-resolved intensity decay.

Considering a fluorophore which displays a single decay time ($\tau$), the time-resolved intensity decay can be described as

$$I(t) = I_0 e^{-t/\tau} \qquad (1)$$

where $I$ is the fluorescent intensity at time $t$ and $I_0$ is the intensity at $t$=0.

Therefore, the relation between the steady-state intensity, $I_{SS}$ and the fluorescent lifetime (decay time) is given by

$$I_{SS} = \int_0^\infty I_0 e^{-t/\tau} dt = I_0 \tau \qquad (2)$$

The value of $I_0$ can be considered to be a parameter that depends on the fluorophore concentration and a number of instrumental parameters. Hence, in molecular terms, the steady-state intensity is proportional to the lifetime (Lakowicz, 1997).

## *2.2 Solvent effects*

The spectra of fluorophores is affected by several environmental parameters such as solvent polarity, specific interactions between the fluorophores and surrounding solvent molecules, pH of the solution, surrounding temperature and the purity of solvent. The adopted idea for the present study is that the solvent polarity influences the emission spectrum. Jablonski energy diagram for fluorescence with solvent relaxation is described in Fig. 1 (Lakowicz, 1997).

Table 1. Absorption and fluorescence wavelength maxima of Nile Blue A. Concentration : $1.0\times10^{-5}$ M (Krihak, 1997).

| Solvent | $\lambda_{max.\ abs.}$ (nm) | $\lambda_{max.\ fluor.}$ (nm) |
|---|---|---|
| Water | 635 ± 1 nm | 674 ± 1 nm |
| Methanol | 626 | 668 |
| Ethanol | 628 | 667 |
| 2-Propanol | 627 | 665 |
| 1-Butanol | 627 | 664 |
| Chloroform | 624 | 647 |

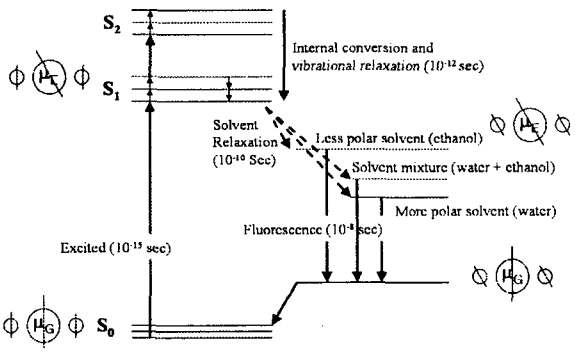


Fig. 1. Jablonski diagram for fluorescence with solvent relaxation. The smaller circles and the lines through them represent the solvent molecules and their dipole moments. Recreated from Ref. (Lakowicz, 1997).

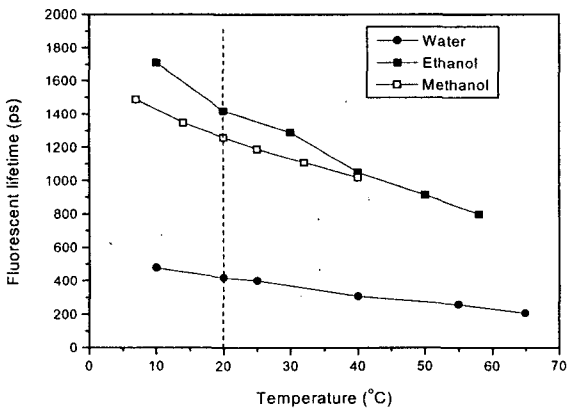


Fig. 2. Changes of fluorescent lifetime in different solvents according to increase of temperature. Recreated plot based on the data presented in Ref. (Kubinyi, 2003).

Solvent effects shift the emission to lower energy region due to the stabilization of the excited state by the polar solvent molecules. Typically, the fluorophore has a larger dipole moment in the excited state than in the ground state. Following excitation, the solvent dipoles can reorient or relax, which lowers the energy of the excited state. As the solvent polarity is increased, this effect becomes larger, resulting in emission at lower energies (quantum yields) or longer wavelengths (Red-shifts or Stokes shift). This effect (general solvent effect) can be accounted by the Lippert equation as given in Eq. (3).

$$\bar{\nu}_A - \bar{\nu}_F = \frac{2}{hc}\left(\frac{\varepsilon - 1}{2\varepsilon + 1} - \frac{n^2 - 1}{2n^2 + 1}\right) - \frac{(\mu_E - \mu_G)^2}{a^3} + constant \qquad (3)$$

In this equation, $\bar{\nu}_A$ and $\bar{\nu}_F$ are the wavenumbers ($cm^{-1}$ ) of the absorption and emission, respectively. And $h$ is Planck's constant, $c$ is the speed of light, $n$ is the refractive index of the solvent, $\varepsilon$ is dielectric constant of the solvent, and $a$ is the radius of the cavity in which the fluorophore resides. This equation describes the energy difference between the ground and the excited state in nonprotic solvent. Nonprotic solvent means that those do not have any groups capable of hydrogen bonding such as hydroxyl groups.

But the theory is often inadequate for explaining the detailed behavior of fluorophores in a variety of environments. This is caused by specific interactions, which are produced by one or more neighboring molecules and are determined by the specific chemical properties of both the fluorophore and the solvent. This specific effects attribute to the hydrogen bonding , acid-base chemistry, or charge-transfer interactions. In addition, there are temperature, pH and density as parameters affecting the fluorescence. Fluorescence intensity usually decreases (not always) with increasing temperature (Lakowicz, (1997), Hercules, (1966)).

The enhancement of the fluorescent signals in micro-LIF measurements can be achieved by using these solvent effects, and then we aim to increase the fluorescence intensity by the addition of EtOH/MeOH with less polarity and low hydrogen bonding relatively to pure water.

### *2.3 Fluorescent intensity signal enhancement of Nile Blue A*

In this study, Nile Blue A ($C_{40}H_{40}N_6O_6S$, Molecular weight: 732.84) was used as fluorophores and dissolved in a mixed solvent. The mixture of water and EtOH (ethanol)/MeOH (methanol) was adopted as a solvent to increase the intensity of fluorescent light since the emission spectrum can be shifted and the fluorescent intensity can be increased or decreased due to addition of a small portion of different solvent (Lakowicz, (1997). Because of the addition of EtOH/MeOH into water, the blue shifts in emission spectrum might be occurred so that the maximum of the emission locates between 674 nm (water) and 667 nm (EtOH/MeOH) (see table 1). Accordingly, the steady state fluorescent lifetime at 20℃ increases from 418 ps (water) to 1420/1280 ps (EtOH/MeOH) as shown in Fig. 2 (Grofcsik et al., (1995), Kubinyi, (2003)). Therefore, considering the linear relationship between the steady-state fluorescence intensity and the fluorescent lifetime in Eq. (2), the fluorescent intensity of the EtOH/MeOH solution can be more than three times higher than that of pure water.

The fluorescence intensity of Nile Blue A was measured by using our micro-LIF measurement system (see Fig. 8). Figure 3 depicts the fluorescent intensity of Nile Blue A (Concentration: 102.3μM) dissolved in water-EtOH (5%) and water-MeOH (5%) solvent mixtures at room temperature (approximately 25℃). This figure demonstrates that the fluorescent intensity was enhanced considerably with addition of EtOH or MeOH, and the intensity for water-EtOH solvent mixture was higher than that for water-MeOH mixture. The fluorescent intensity signal in water with 5% ethanol was enhanced to 43% over that in pure water, and in water with 5% MeOH, to 28%. These intensity increases were resulted from the decreased polarity due to the addition of EtOH or MeOH with lower polarity than water (general solvent effect) and from the lower hydrogen bonding (specific solvent effect) as discussed in the previous section (Lakowicz, (1997), Hercules, (1966)).

Volume fraction of EtOH versus fluorescent intensity for each concentration of Nile Blue A is described in Fig. 4. It shows the fluorescent intensities of dye in the solvent mixture are increased according to the volume fraction of EtOH. A non-linearity is observed in the higher concentration range.

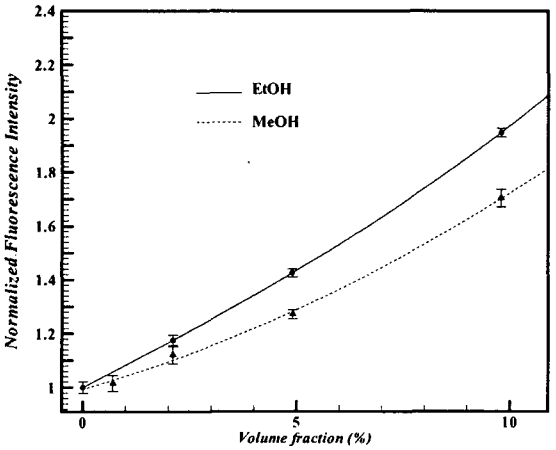


Fig. 3. The fluorescence intensity variation of Nile Blue A in solvent mixtures of water-EtOH and MeOH according to various volume fractions of EtOH or MeOH at the mixture temperature of 25□ (C = 102.3 μM). The fluorescent intensity signal in water with 5% EtOH was enhanced to 43% over that in pure water, and in water with 5% MeOH , to 28%.

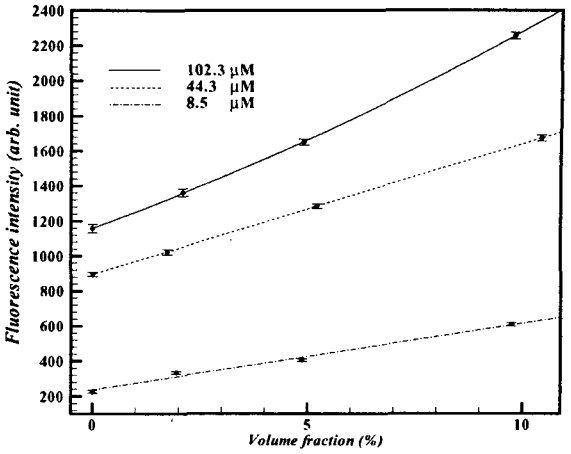


Fig. 4. Volume fraction of EtOH versus fluorescent intensity according to each concentration of nile blue A in solvent mixtures of water-EtOH/MeOH at 25□. The concentrations were 102.3μM (solid line), 44.3μM (dash line) and 8.5μM (dash-dot line).

# 3. Micro-LIF Measurement Method with Micro Laser sheet Illumination

## *3.1 Micro laser sheet*

In addition to the novel idea of using a solvent mixture to substantially increase the fluorescence lifetime or the steady-state emission intensity, the second important idea of this research is the use of a micro laser sheet generator associated with a diode laser. The Gaussian-to-flat-top laser intensity profile was accomplished by a Powell lens in the line generator (StockerYale, Inc.). Figure 5 shows the test data sheet of the configuration of the laser focusing. The thickness of laser light is 2.8μm at the 50% of maximum intensity and 5.3μm at the 13.5% of maximum intensity, respectively. The Rayleigh range and the depth of focus can be calculated by using Eq. (4). The Rayleigh range ($Z_R$) is defined as the distance over which the thickness of the line has increased by a factor of square root of 2 ($\sqrt{2}$). And the depth of focus is defined as twice of Rayleigh range ($2Z_R$).

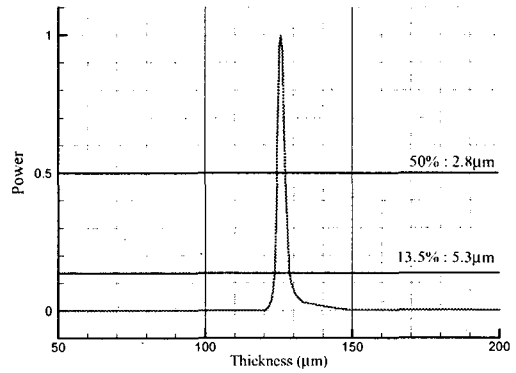


Fig. 5. Micro laser sheet test-data showing the thickness of Laser sheet at 50% of peak power measured to be 2.8μm and at 13.5% of peak power, 5.3μm (StockerYale, Inc.)

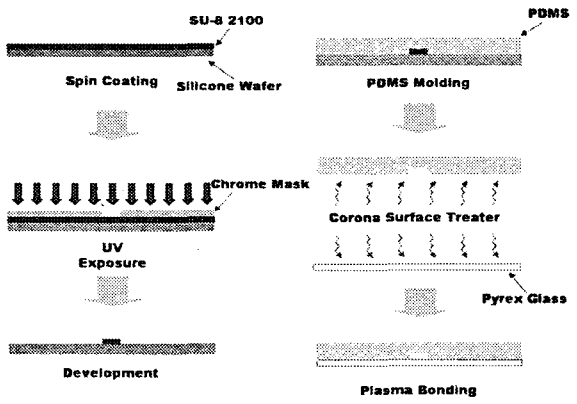


Fig. 6. Fabrication process of micro-channel.

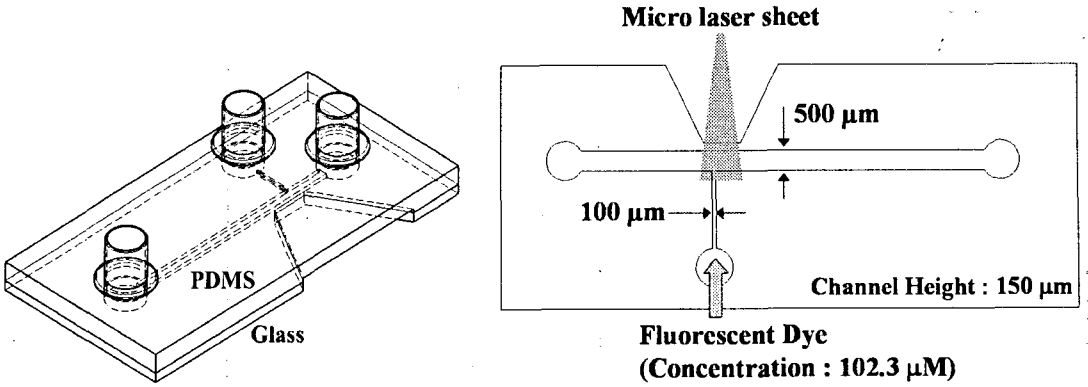


Fig. 7. Shape and dimension of micro-channel.

$$2Z_R = \frac{2\times\pi\times B^2}{\lambda\times 4} \qquad (4)$$

where $B$ is the minimum line width and $\lambda$ denotes the laser wave length. The micro laser sheet generator has about 70μm of the depth of focus which corresponds to the area having 1.4 times of minimum beam thickness. It means that the thickness of laser sheet beam is less than 7μm within ±35μm from the beam focus. When the laser sheet is used to a micro-channel with 100μm width, the flow is illuminated with less than 10μm depthwise resolution of the laser sheet beam thickness.

### *3.2 Microchannel design and fabrication for micro-LIF*

The microchannel used in this study was made of PDMS (Polydimethylsiloxane) (Dow Corning Corp.) and the channel was bonded with a glass plate. Figure 6 illuminates the fabrication process of a micro-channel following a general MEMS fabrication process. The channel pattern of 150μm high was constructed by the spin coating process using highly viscous photo resist, SU-2100 (MicroChem corp.), then the coated photoresist covered by the chrome mask is exposed by a UV beam and moved to the development process. Then the gell-like PDMS is poured on top of the positively patterned photoresist layer to fabricate PDMS molding of a microchannel. After this PDMS molding, a Pyrex glass is bonded to PDMS by means of plasma bonding using a corona surface treater. The chrome mask, in lieu of the conventional photographic negative mask, was used to create well-defined channel wall and deeper channel height.

Figure 7 demonstrates the shape and dimension of the micro-channel used in this experiment. To minimize the distortion and refraction of the laser sheet and to ensure an easy access of the thin laser sheet to the micro-channel, the side part of the molded PDMS is cut to a "wedge" shape so that the PDMS wall thickness can be as small as 200μm. The channel consists of 500μm wide main channel and 100μm wide side channel for fluorescent dye injection. The channel height is 150μm for both channel sections.

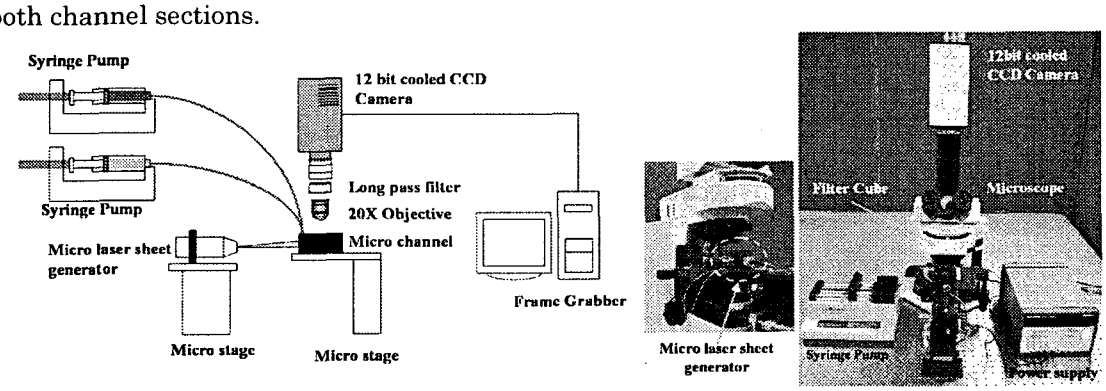


Fig. 8. Experimental setup for μ-LIF measurement.

### *3.3 Experimental setup*

Figure 8 depicts the schematic illustration of experimental setup and photographs of the experimental apparatus. The developed μ-LIF system consists of a 12 bit cooled CCD camera, a microscope equipped with a long pass filter cube, micro laser line generator and syringe pumps. To reduce measurement errors due to dark noise, a Peltier cooled CCD camera has been used. To positioning and scanning of the micro laser sheet, a three-axis micro-traversing stage and a three-axis tilting stage have been used. An appropriate fluorescence dye had to be selected to be best matched with the 638 nm laser wave as an absorption band. The candidate fluorescence dyes were Nile Blue A, Alexa Fluor 633, TOTO 3 and Oxazine 170. We chose Nile Blue A since it is widely used in biology and material science. Nile Blue A has 635nm of the maximum excitation wavelength and 675 nm of the maximum emission wavelength in water solution. Because of the relatively wide separation between the absorption and emission bands, the emission band filtering can be more discrete. The base color of Nile Blue A is blue in the day light, whereas it emits red at 675 nm when the laser absorption at 635 nm peak is taking place. To enhance the fluorescence intensity by the use of the aforementioned solvent effect, 5% volume fraction of ethanol was added for all experiment.

A long pass filter with 665 nm cut-off was used to block out the illuminating laser light with a peak intensity at 638 nm. The fluorescence light at 675 nm wavelength passes through the filter with 90% of transparency ratio, while the illuminating laser light of 638nm is completely eliminated with less than 0.01% of transparency ratio.

### *3.4 Pixel-by-pixel calibration of fluorescence intensity versus the dye concentration*

An elaborate pixel-by-pixel calibration is necessary to obtain accurate quantitative concentration fields. The calibration was performed for several concentrations of the dye dissolved in the solvent mixture of water (95%) and EtOH (5%). With the micro laser sheet beam illumination into the micro-channel, 20 images were acquired for each concentration case, and then averaged for each pixel. Then the averaged fluorescent light intensity (image intensity) fields were used to get the calibration coefficients. A 4th order polynomial function was adopted as the fitting function, and the method of least squares was used as follows;

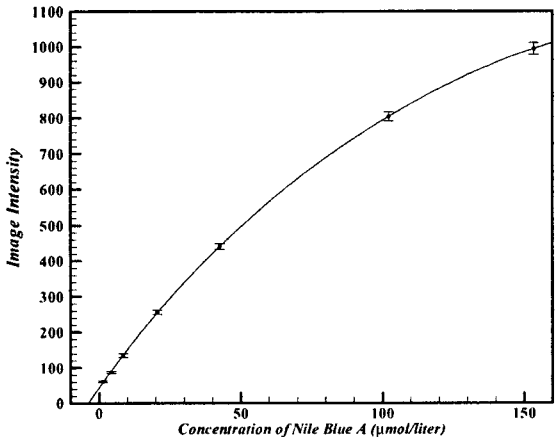


Fig. 9. 1×1 Calibration data and curve fit at (560,560) on the calibration image plane. 20 images were acquired and averaged at each concentration case of 1.3, 4.3, 8.5, 20.5, 42.6, 102.3, 153.5 μM at each pixel. The solid curve shows a least square fitting by a 4-th order polynomial function.

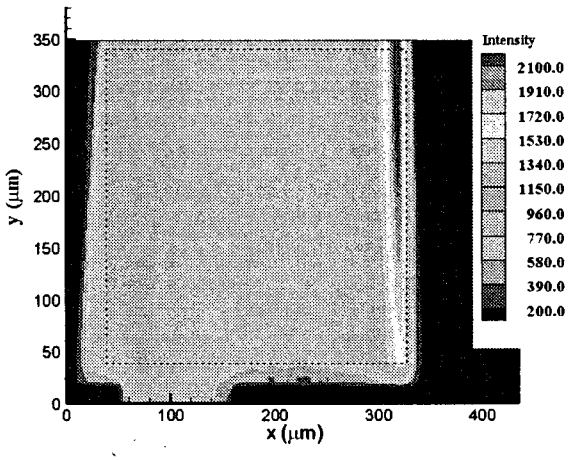


Fig. 10 Uncalibrated fluorescence intensity field with constant volume concentration of Nile Blue A dissolved in water (95%)-EtOH (5%).

$$C(I) = a_{0_{(i,j)}} + a_{1_{(i,j)}} I_{(i,j)} + a_{2_{(i,j)}} I^2_{(i,j)} + a_{3_{(i,j)}} I^3_{(i,j)} + a_{4_{(i,j)}} I^4_{(i,j)} \quad (5)$$

where $C$ is concentration value, $I$ is fluorescent intensity value and $a_m$ is coefficients to be determined, and $(i, j)$ denotes the location in the image plane or the pixel location. Since the calibration procedure was performed for each pixel in the whole image plane, about 1 million of calibration functions were obtained and used to calculate concentration values. The lateral spatial resolution of concentration field was estimated to be about 340nm which is the physical size corresponding to one image pixel.

Figure 9 shows the resulting calibration curve of Nile Blue A volume concentration versus the fluorescent light intensity at a selected pixel location at $i$ = 560, $j$ = 560 of the image plane. The fourth-order polynomial calibration curve is well fitted with the calibration data at each pixel. The calibration curve shows a non-linear behavior, but linearity is observed in the lower concentration range.

### *3.5 Evaluation of micro-LIF measurement using micro laser sheet beam*

To qualitatively determine the concentration field, the pixel-by-pixel calibration functions were applied to the instantaneous fluorescent image with a known concentration of 102.3μM. Figure 10 shows the contour plot of the uncalibrated intensity of instantaneous fluorescent image. Although the injected fluid has the uniform concentration value, the recorded fluorescent intensity shows wide variation due to the background non-uniformity of the incident laser light intensity and other non-uniformities associated with the CCD recordings. Figure 11 shows the calibrated instantaneous concentration field from the raw image shown within the square dashed region in Fig. 10 and the probability density distributions and cumulative density distributions of measured concentration values are shown for three different spatial resolution of 1×1 (Fig. 11-a), 3×3 (Fig. 11-b) and 5×5 (Fig. 11-c) pixel dimensions. To minimize the intensity fluctuations resulted from the CCD random noise, and also to improve the pixel-by-pixel intensity uncertainties, the grid size of investigation window was varied from 1×1, 3×3 to 5×5 pixels, with their corresponding spatial resolutions of 0.34μm×0.34μm to 1.03μm×1.03μm, 1.72μm×1.72μm. The concentration uniformity is substantially enhanced with increasing spatial resolution. Most of the calibrated concentration values are fluctuating about 102.3μM within a few percent and generally in a good agreement with the real value (102.3μM). The values of error seem to be distributed randomly and they persistently decrease with increasing spatial resolution. This suggests that the most errors are caused by the fluctuation of fluorescence image intensity from the CCD camera while the volume concentration remains constant. The RMS errors between the specified concentration and the calibrated measured values are estimated as 2.69 μM (relative error: 2.63%) for 1×1 pixel size, 0.94 μM (0.89%) for 3×3 pixels size and 0.56 μM (0.54%) for 5×5 pixels size. From the probability distribution and cumulative distribution functions, 95% of total data points have 5% or less relative errors for the 1×1 pixel resolution, 97% data points have less than 2% relative errors for the 3×3 pixel resolution, and 94% data points have less than 1% relative errors for the 5×5 pixel resolution. The RMS errors show dramatic reductions with increasing spatial resolution from 0.34μm to 1.72μm square.

## 4. Conclusion

The fluorescent intensity signal for micro-LIF measurements was successfully enhanced from the addition of small portion of a different solvent with low polarity. This novel use of low-polarity solvents seems to be a highly formidable to enhance the signal-to-noise ratio for general LIF measurements. The fluorescence of Nile blue A was substantially increased by the use of a solvent mixture of water and EtOH/MeOH at low volume concentration of 5% or less. Micro-LIF method using a micro laser sheet beam of about 5μm thick was developed and applied to a microchannel with about 150μm height. The use of the elaborate pixel-by-pixel calibration confirms that the accurate concentration fields can be determined by using a micro-LIF method with micro laser sheet beam. The inherent rms errors resulted from the CCD noise and other imaging

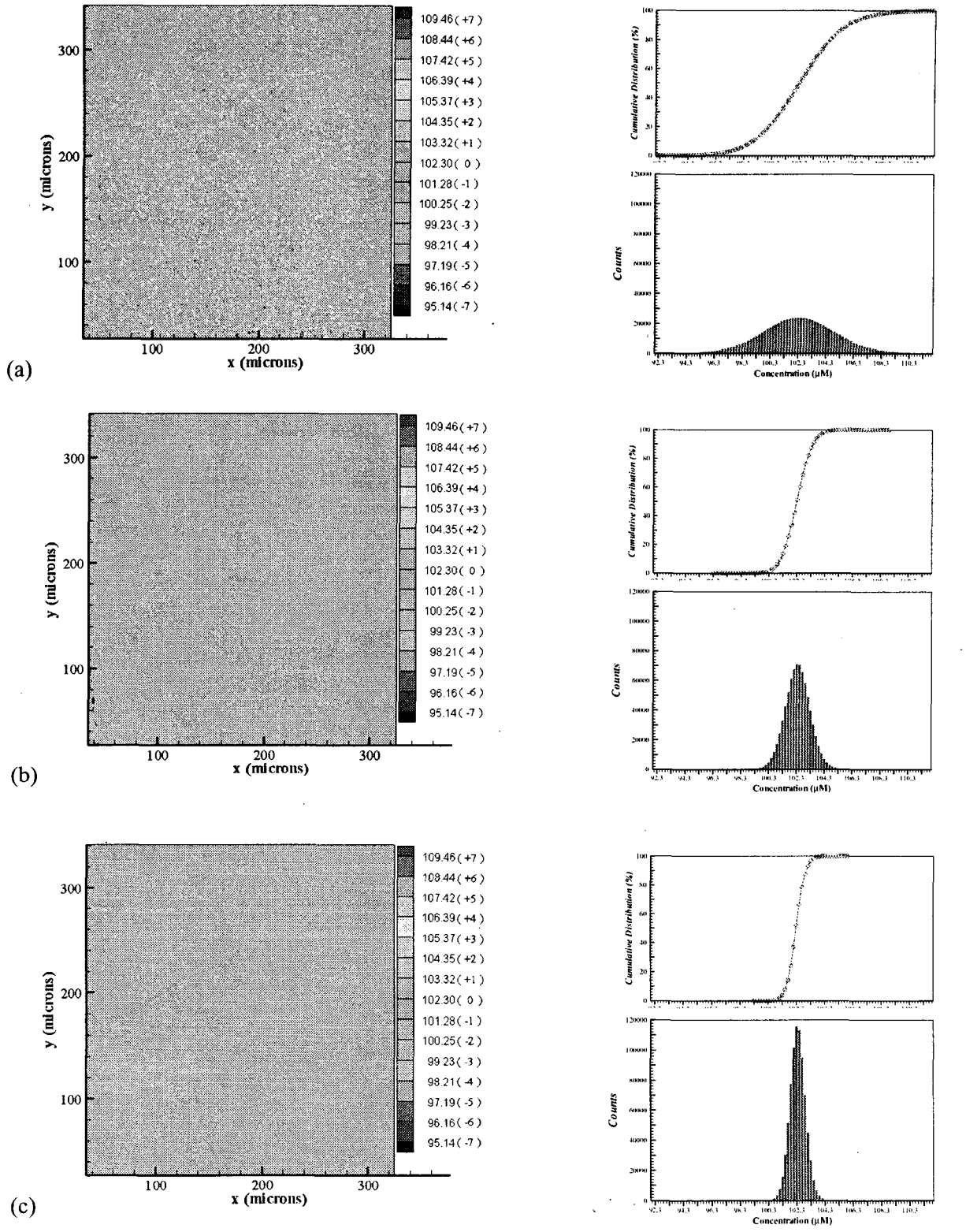


Fig. 11 Concentration values (μM) calculated from Fig. 10 using the pixel-by-pixel calibration and their relative errors (%) are described in the parentheses next to the concentrations. The cumulative distributions and the probability densities are also shown for three spatial resolutions: (a) 1×1, (b) 3×3, (c) 5×5 pixel dimensions. 95% of total values have less than 5% relative errors at 1×1pixel size, 97% of total values have less than 2% relative errors at 3×3 pixels size, and 94% of total values have less than 1% relative errors at 5×5pixels size.

sources can also be reduced by increasing the interrogation grid sizes, from 1×1 to 3×3 to 5×5 pixels, equivalently 0.34μm×0.34μm, 1.03μm×1.03μm, to 1.72μm×1.72μm spatial resolution.

## *References*


Kim D.S., Kang T.G., Lee S.W., Kwon T.H., "Experimental and Numerical Characterizations of Barrier Embedded Micromixer," Proc., μTAS 2003, (2003) pp. 121-124.

Glasgow I. and Aubry N., "Pulsed Flow Mixing for Biomems Applications," Proc., μTAS 2003, (2003), pp. 125-129.

Suzuki H. and Ho C.M., "A Magnetic Force Driven Chaotic Micro-Mixer," Proc., the 15th IEEE International Conference on MEMS (MEMS 2002), (2002), pp. 40-43.

Shinohara K., Sugii Y., Okamoto K., Hibara A., Tokeshi M., Kitamori T., "Micro-PIV and Micro-LIF Measurements of Chemically Reacting Flow in Micro Fluidic Device," Proc., 5th Int. Sym. on Particle Image Velocimetry, (2003), Paper No. 3238.

Grofcsik A., Kubinyi M., Jones W.J., "Fluorescence Decay Dynamics of Organic Dye Molecules in Solution," J. of Molecular Structure, 348, (1995), pp. 197-200.

Kubinyi M., Grofcsik A., Papai I., Jones W.J., "Rotational Reorientation Dynamics of Nile Blue A and Oxazine 720 in Protic solvents," Chemical Physics, 286, (2003), pp. 81-96.

Krihak M., Murtagh M.T., Shahriari M.R., "A Spectroscopic Study of the Effects of Various Solvents and Sol-Gel Hosts on the Chemical and Photochemical Properties of Thionin and Nile Blue A," J. of Sol-Gel Science and Technology, 10, (1997), pp. 153-163.

Ghanadzadeh A., Tajalli H., Zirack P., Shirdel J., "On the photo-physical behavior and electro-optical effect of oxazine dye in anisotropic host," Spectrochimica Acta Part A, vol. 60, (2004), pp. 2925-2932.

Lakowicz R.J., "Principles of Fluorescence Spectroscopy,", 2nd Edition, Plenum press, (1997), New York.

Hercules, D. M., "Fluorescence and Phosphorescence Analysis ; Principles and Applications," Int. Edition 18,(1966), Univ. of Tokyo Press, Tokyo.

Koti A. S. R., Periasamy N., "Solvent Exchange in Excited-State Relaxation in Mixed Solvents," J. of Fluorescence, Vol. 10, No. 2, (2000), pp. 177-184.

Mondal M., Chakrabarti A., Basak S., "Photophysical Study of Local Anesthetics in Reverse Micelles and Water-Ethanol Mixtures," J. of Fluorescence, Vol. 13, No. 4, (2003), pp. 307-314.

Das. K., Jain B., Patel H. S., "Nile Blue in Triton-X/Benzene-Hexane Reverse Micelles: a Fluorescence Spectroscopic Study," Spectrochimica Acta Part A, 60, (2004), pp. 2059-2064.

Tran Y., and Whitten J. E., "Using a Diode Laser for Laser-Induced Fluorescence," J. of Chemical Education, Vol. 78, No.82, (2001), pp. 1093-1095.